17th World Conference on Earthquake Engineering, 17WCEE
Sendai, Japan - September 13th to 18th 2020

DAMAGE ESTIMATION OF RC MEMBER CONSIDERING AN EFFECT OF STRAIN RATIO AND DISTRIBUTION ON CRACK PROPAGATION

N. Takahashi[(1)]

[(1)] *Associate Professor, Tohoku University, ntaka@archi.tohoku.ac.jp*

Abstract

Damage of RC members obtained from static loading experiments is different from the damage of that observed after real earthquakes. The reason is that the difference in not only the displacement history but also the loading ratio affects the cracking propagation process and mechanism. The purpose in this research is to develop and apply seismic damage evaluation considering the damage propagation process and mechanism of RC members to the performance-based seismic design, rather than the seismic damage evaluation method of RC members based on the statistical results of static loading experiments. Therefore, a simple method for estimating the quantitative earthquake damage according to the demand or response of structural member in a typical seismic design is investigated.

To analyze the damage propagation process and mechanism of RC members to the performance-based seismic design, RC beams experiment with different loading ratio is carried out. And the effects of loading ratio on the crack length, the crack spacing, and the surface strain distribution in the vicinity of crack growth and propagation are examined from the experimental results. Then, the digital image correlation method (DIC) is applied to the measurement of the surface strain distribution where the discontinuous area which crosses the crack is also included. At the same time, the optimal facet size is studied because the optimal size of DIC might be different from the case of application to the continuum materials.

Through the above-mentioned investigation, the following results are concluded.

(1) When DIC is applied to strain distribution measurement nearby cracks occurring on the concrete surfaces, the optimal facet size is 0.5 times the strain gauge length. That brings the most approximate measurement results by strain gauge as a conventional method.

(2) Before the steady-state crack propagation, the tensile force and strain occurs on the concrete in the vicinity of the hair crack. After the steady-state crack propagation, the crack widens like between rigid elements.

(3) A method to change the average crack spacing according to the rebar strain distribution is proposed. By determining the relationship between the occurrence of primary cracks and secondary cracks and the rebar strain distribution, it is possible to roughly estimate the amount of crack damage after an earthquake.

(4) The strain under the dynamic loading is concentrated rather than that under static loading after a steady-state crack propagation.

Keywords: RC, crack propagation, strain distribution, loading ratio, digital image correlation

1. Introduction

Damage of RC members obtained from static loading experiments is different from the damage of that observed after real earthquakes. The reason is that the difference in not only the displacement history but also the loading ratio affects the cracking propagation process and mechanism. The purpose in this research is to develop and apply seismic damage evaluation considering the damage propagation process and mechanism of RC members to the performance-based seismic design, rather than the seismic damage evaluation method of RC members based on the statistical results of static loading experiments. Therefore, a simple method for estimating the quantitative earthquake damage according to the demand or response of structural member in a typical seismic design was investigated.

To analyze the damage propagation process and mechanism of RC members to the performance-based seismic design, RC beams experiment with different loading ratio is carried out. And the effects of loading ratio on the crack length, the crack spacing, and the surface strain distribution in the vicinity of crack growth and propagation are examined from the experimental results. Furthermore, to clarify the crack propagation mechanism, not only the strain of rebars but also that of concrete surface needs to be analyzed. But using strain gauge cannot be appropriate measurement method for the full-field strains on concrete surface. Then, the digital image correlation method (DIC) is applied to the measurement of the surface strain distribution where the discontinuous area which crosses the crack was also included. At the same time, the optimal facet size is studied because the optimal size of DIC might be different from the case of application to the continuum materials.

Additionally, to estimate the damage of R/C structure under seismic load with simply method, two full scale reinforced concrete beam specimens with same size is tested under static load and dynamic load on shaking table, and the effect of strain distribution is discussed. The result of this discussion is introduced into the damage estimation method which combined with the empirical and mechanical models, and simple method of estimating the crack propagation considering strain distribution and effect of strain rate is proposed. Proposed method of estimating the crack propagation of full scale 4-story reinforced concrete structure members under seismic load is verified in this research.

2. Optimal parameter for obtaining the strain nearby cracks using DIC

2.1 Outline of Four-point flexural test for RC beam

The larger facet-size generally gives the more accurate strain as far as focusing on continuous materials such as steel. On the other hand, in the case of analyzing the relationship between the cracks and strains on concrete surface, the larger facet-size is not appropriate for obtaining the strain. The excessive smoothing could occur in the area where the multiple cracks are observed such as shown in Figure 1.

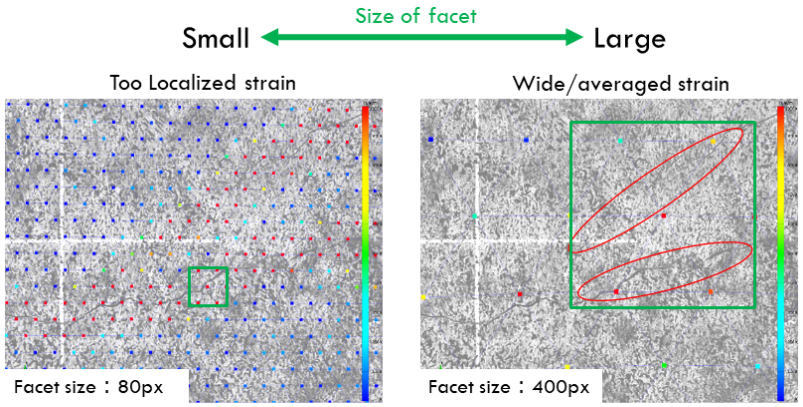

Figure 1 – Examples of employing the different facet sizes（0.22mm/pixel）

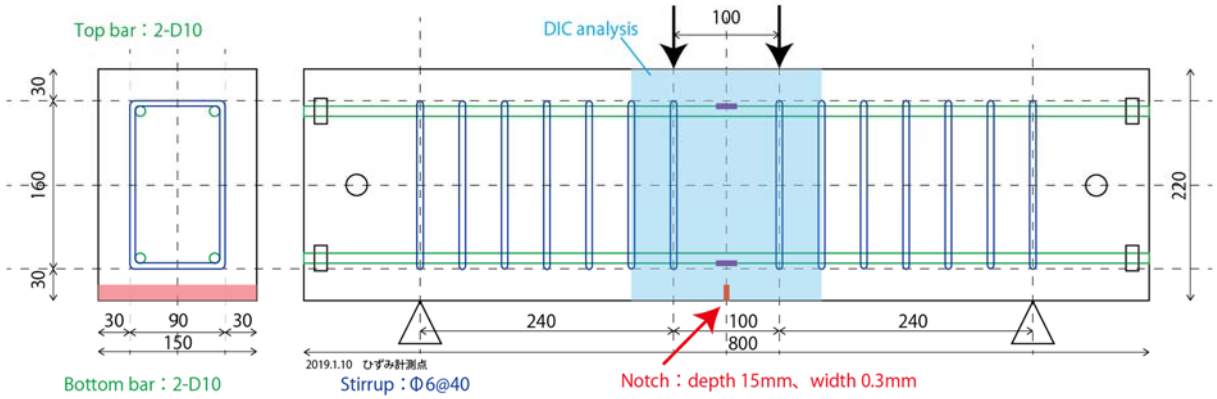

(a) RC beam specimen detail

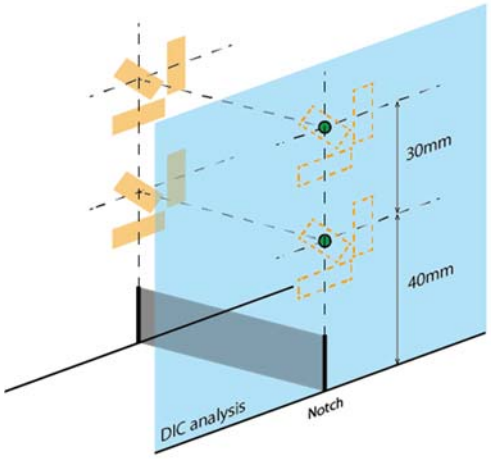

(b) DIC analysis field

Figure 2 – The notch provided RC beam

Therefore, the optimal facet-size for DIC is estimated through the 4-point flexural test for RC specimen having small notch (Figure 2). Material property of RC beam specimen is shown in Table 1. Parameters of 4-point flexural test with DIC is shown in Table 2. Based on the previous research and literature [1], the speckle with 3 to 5 pixels of the camera resolution is preferred as the minimum speckle size. In addition, the optimal distance between facets for DIC analysis is 0.8 times the size of the facet size. In this research, these conditions are employed to the all experiment.

Table 1 – Material Property

$B \times D \times L$ [mm]		150 × 220 × 800 Notch in position of L=400
Steel	Rebar	2-D10 (SD295A)
	Reinforcement	SR235@40
Concrete	σ_B [MPa]	26.1
	E_C [MPa]	23300
	σ_T [MPa]	10.2

Table 2 – Parameters of 4-point Flexural Test with DIC

No.	Loading rate [mm/min]	Video camera pixels [Pixel]	Resolution [mm/pixel]	Facet size [Pixel]	Distance between facets [Pixel]	Speckle size [mm]	Video image clipping interval [s]
1	3.6	3840 x 2160	0.2037	25	20	0.6 to 1.0	1
2			0.0769	65	52	0.2 to 0.4	
3	72		0.2024	25	20	0.6 to 1.0	0.1
4							

2.2 Verifying the optimal facet-size with cracking

(1) Limits of facet-size

Facet-size is normalized as the "gauge length ratio" unit which is calculated as the ratio of facet-size to strain gauge length. In this research, the employed strain gauge has the same length as 10mm. The lower limit of facet-size to be able to obtain the strain by DIC is estimated as the gauge length ratio of 0.3, but the accuracy is too low as shown in Table 3. The higher limit of facet-size to obtain the strain does not exist, but the larger gauge length ratio decreases the accuracy as shown in Table 3. It implies that the facet-size which is larger than gauge length provides excessive smoothing of local strain nearby cracks and it can be said that it is not appropriate for measuring strain nearby cracks on concrete surface.

Table 3 – The relative error of principal strain between DIC and strain gauge

Gauge Length Ratio	Specimen No.2	Specimen No.4
0.3	240%	70%
0.4	64%	58%
0.5	-2%	8%
0.6	-9%	22%
0.8	-34%	-3%
1	-46%	-33%
1.2	-55%	-39%
2	-64%	-62%

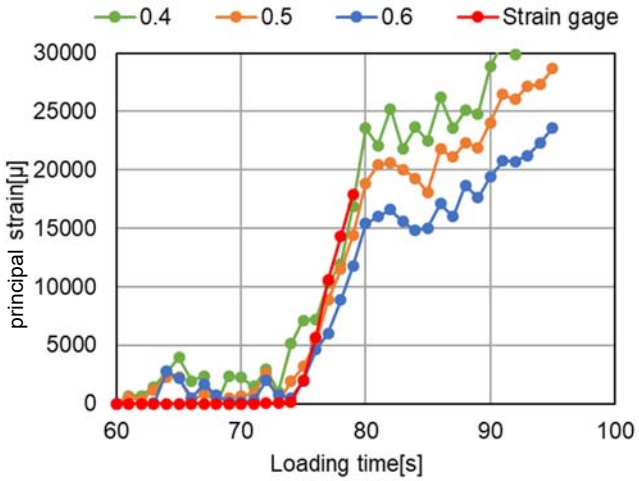

Figure 3 – Result of each "gauge length ratio" as facet-size employed in DIC

(2) Optimal facet-size

Figure 3 shows the principal strain obtained from 4-point flexural test employing DIC with different facet-size. As a result, the strain by DIC with the gauge length ratio of 0.5 as facet-size approximates the strain gauge measurement result. It means that using 0.5 times of gauge length as the facet-size gives the closest result to the conventional measuring method using strain gauges. It is important to note that if inappropriate facet-size is used to DIC analysis, the result may not be appropriate enough to compare with strain gauge measurement result.

2.3 Discussion for the relation between concrete strain and crack width

To discuss the relation between concrete strain and crack width, the idea of "rigid-body crack strain" is employed. Figure 4 shows the schematic of rigid-body crack strain. The calculated strain in DIC is generally consist of concrete strain and crack width. The "rigid-body crack strain" is assumed that the obtained strain is calculated by only the crack width without concrete strain.

DIC and crack width measurement point is set on where flexural cracks and flexural-shear cracks occurred as shown in Figure 5.

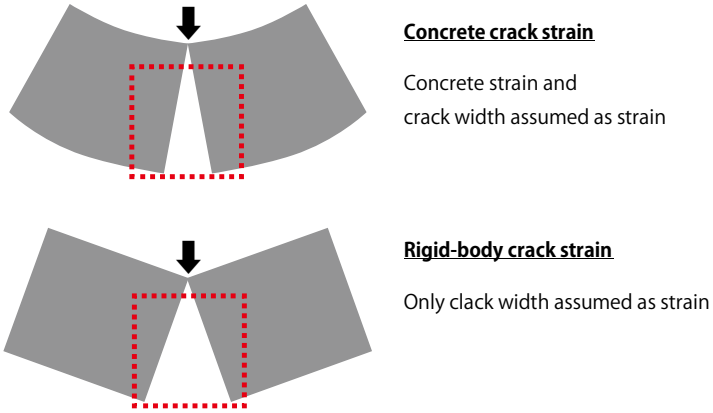

Figure 4 – Schematic of "rigid-body crack strain"

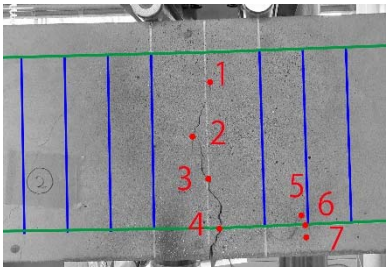

Figure 5 – Measurement points

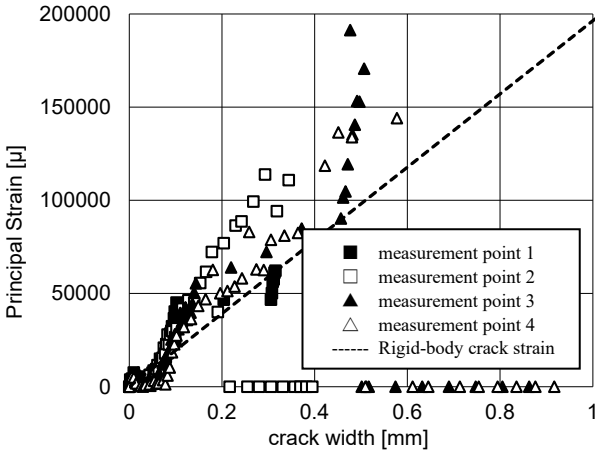

Figure 6 – Principal strain vs. Flexural crack width

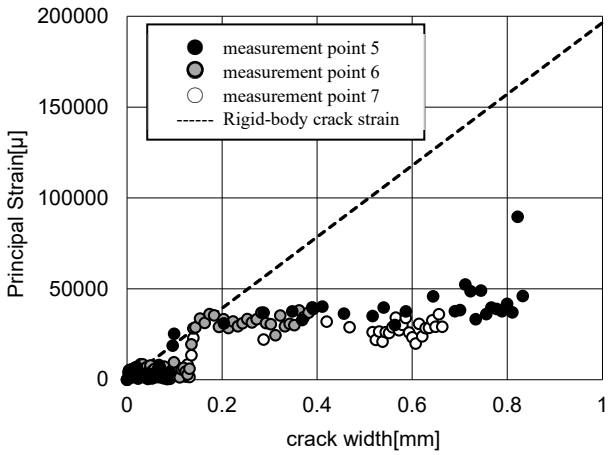

Figure 7 – Principal strain vs. Flexural-shear crack width

For flexural cracks, when the crack width is larger than 0.2 mm, the slope of the plot is almost equal to the slope of the rigid-body crack strain. In this stage, the cracks widened while the concrete tensile strain remained almost unchanged. This implies that the adhesion between the concrete near the crack and the rebar deteriorates, and the tensile stress is not transmitted to the concrete surface. When the crack width is increased and the crack width exceeds 0.3 mm, the tensile strain of the concrete occurs again, and the slope of the plot in the figure becomes larger than the slope of the rigid crack strain (Figure 6). The increment of stress from the part where the adhesion between the concrete and the main reinforcement has not deteriorated has been transmitted to the concrete surface.

As for the flexural-shear cracks, the strain increases as the crack width approached 0.2 mm. When the crack width is over 0.2 mm, the principal strain is almost stable and only the crack width tended to widen (Figure 7). It is considered that the increase in flexural tensile strain and the compressive strain due to the shear resistance mechanism influenced each other.

Figure 8 and 9 shows the relationship between principal strain and flexural crack width (measurement point 4) in static loading and dynamic loading, respectively. Both figures indicate almost the same trend, but the result of dynamic loading in Figure 9 shows more like a flexural-shear crack trend. When the crack width is under 0.2 mm, the tensile force and strain occurs on the concrete in the vicinity of the crack. After the crack width growth over 0.2mm and steady-state of crack propagation, the crack seems to widen without tensile strain on the concrete.

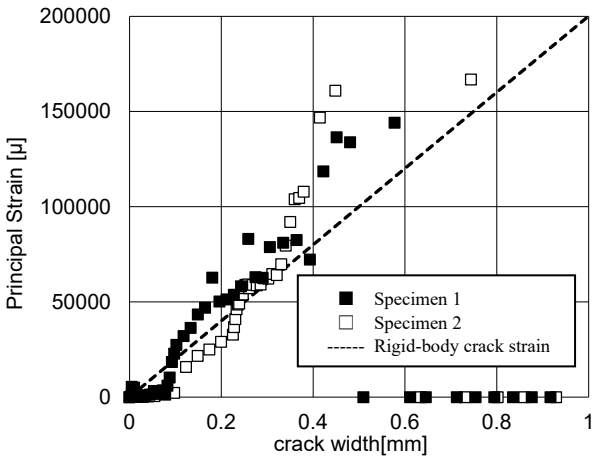

Figure 8 – Strain vs. Crack width in static loading

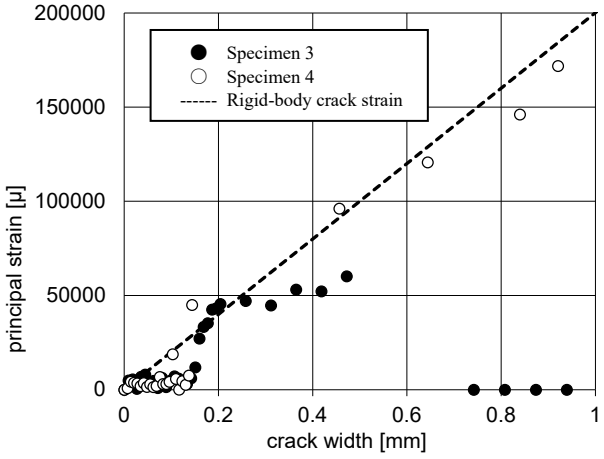

Figure 9 – Strain vs. Crack width in dynamic loading

3. Applying DIC technic to shaking table test

3.1 Outline of the shaking table test for RC sub-assemblages

The static and dynamic loading tests for 2 full-scale RC sub-assemblages are carried out using a shaking table (Figure 10). To avoid self-vibration and dust from spalling area, the equipment consists of 4K action camera with protection cover settled directly on the shaking table (Figure 11).

Figure 10－Shaking table test

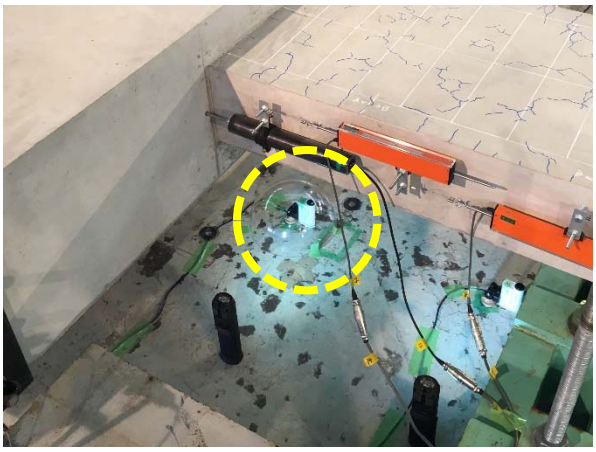

Figure 11－Applying DIC to shaking table test

Material property of RC sub-assemblages is shown in Table 4. Test setup is shown in Figure 12. RC sub-assemblages' detail is shown in Figure 13. Loading protocol of static test is shown in Figure 14, and loading protocol of dynamic test is shown in Figure 15. The wave employed for static loading test is a sine wave with a period of 100 seconds. The wave employed for the dynamic loading test is also a sine wave with a period of 1 second.

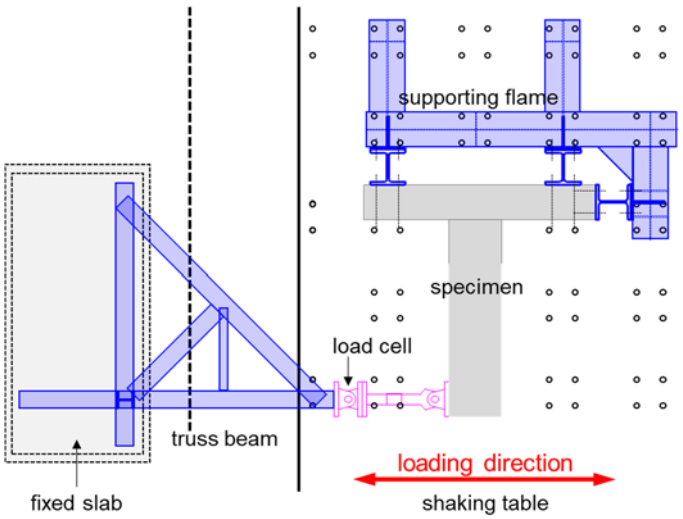

Figure 12－Test setup

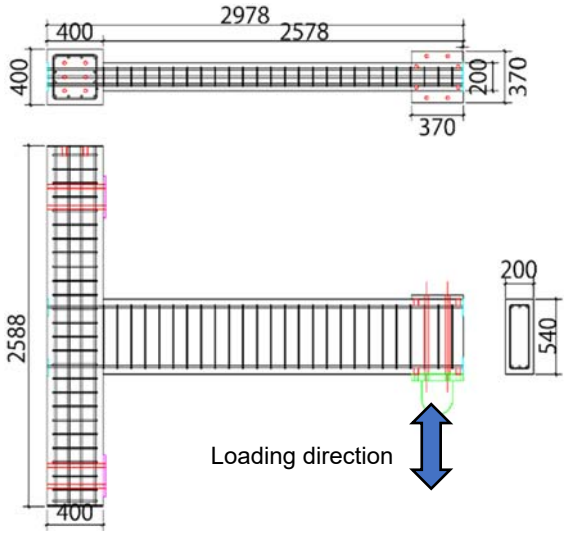

Figure 13－RC sub-assemblages specimen detail

Table 4－Material property

Beam [mm]	$B \times D$	200×540
	Rebar	3-D16(SD390)
	Stirrup	D6(SD295)@100
Column [mm]	$B \times D$	400×400
	Rebar	12-D16(SD390)
	Hoop	D10(SD295)@100
Concrete [MPa]	σ_B	21.4
	E_c	21800
	σ_T	1.55

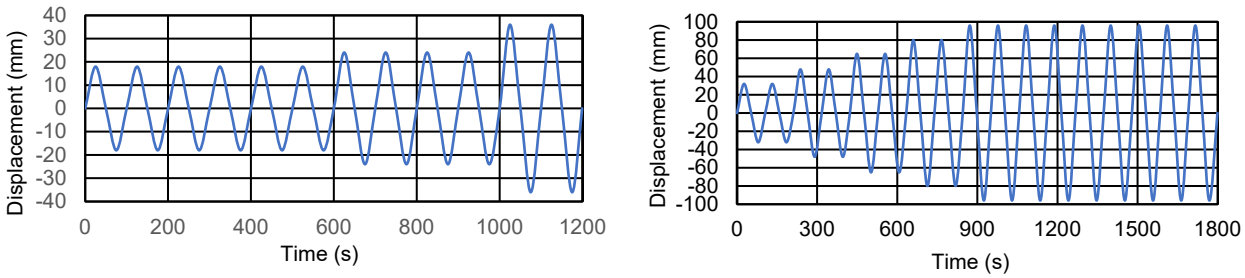

Figure 14－Loading protocol of static test

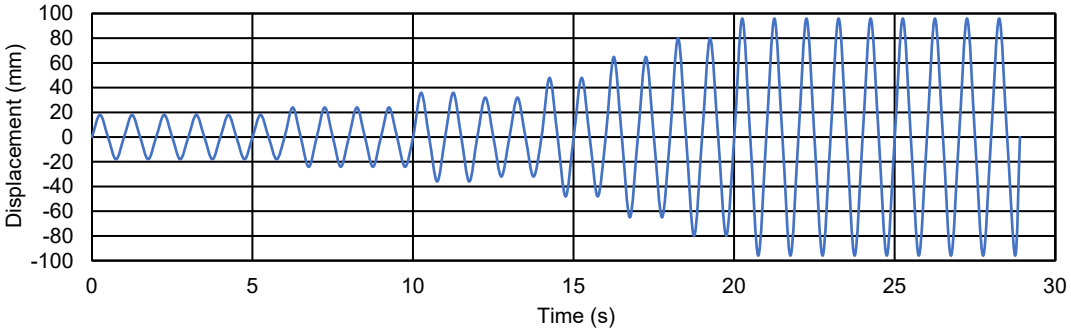

Figure 15－Loading protocol of dynamic test

3.2 Results of the relation between concrete strain and crack width

The relation between concrete strain and crack width is shown in Figure 16. The crack width has calculated with the accuracy due to the digital image resolution (1pixel = 0.22mm). In both specimens, a different trend is observed in the relationship between strain and crack width before and after the crack saturation state. In this research, the crack saturation state means that new crack generation is not occurred anymore.

The black dotted line in Figure 16 represents the rigid-body crack strain. Both graphs show that the slopes are larger than the black dotted line before the crack saturation state. During the crack saturation state, the slopes get closer to the black dotted line.

It implies that the concrete nearby crack has a tension stress and strain before the crack saturation state, and concrete nearby crack loses a tension stress and strain after reaching the crack saturation state. It means that the bond stress between concrete and reinforcing bar nearby crack is completely lost and it is similar to the discussion in the previous chapter.

In this shaking table test, the crack width just before the crack saturation state is 0.5mm under static loading, and 0.8mm under dynamic loading. The specimen under dynamic loading needs a larger crack width to reach the crack saturation state than that of under static loading.

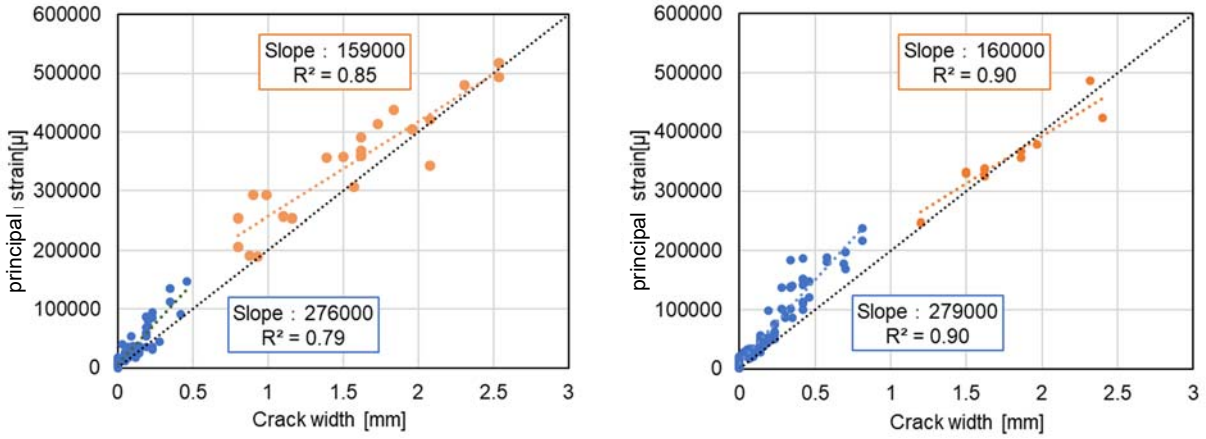

(a) Static loading specimen (b) Dynamic loading specimen

Figure 16－ Relation between concrete strain and crack width

4. Crack propagation mechanism considering loading rate and strain distribution

4.1 Damage estimation method combining the empirical and mechanical models

In damage estimation method proposed by former research [2], the moment distribution of an R/C structural member can be described as triangle distribution under the inflection point. Flexural cracks generate at the extreme tension fiber where the moment M is larger than flexural cracking moment M_c. This cracking zone, which length is defined as l_{cr}, is expressed as Equation (1).

$$l_{cr} = \left(1 - \frac{M_c}{M}\right) H \tag{1}$$

Where, H: shear span. The number of flexural cracks is also expressed as Equation (2).

$$n = 1 + \frac{l_{cr}}{S_{av}} \tag{2}$$

Where, S_{av}: Average flexural cracking space. The length of flexural crack is defined as the distance from the extreme tension fiber to the point of concrete tensile strength estimated from a fiber model analysis.

The flexural-shear cracks propagate after the flexural cracks extending in the plastic hinge area when the angle of principal stress to the axis of the beam calculated from Mohr's stress circle comes under 75 degrees at the end of flexural cracks. When the shear force is larger than shear cracking strength, shear cracks are generated on the preserved discrete line which excludes the plastic hinge area. These shear cracks have an average shear crack space.

4.2 Damage estimation method considering the effects of strain distribution and strain rate

In the above-mentioned method, the effects of steel bar's plasticizing and the increase of the strength of materials caused by increase of strain rate is not considered. Based on the result of the damage of beam specimens under static load and dynamic load, the average cracking space after the yielding decreases to half of the value before yielding. This phenomenon is confirmed through the previous experimental result [3]. Additionally, the increase of strain under dynamic load is more concentrated at the area where steel bar get yield comparing with the specimens under static load through the previous experimental result [3].

In this paper, the average flexural cracking space proposed by former research [4] are assumed to be the average flexural cracking space S_{av}. S_{av} is used to describe the average flexural cracking space in crack saturation state, and the relationship between the average flexural cracking space of the cracks before crack saturation state S_{av1} and after crack saturation state S_{av2} are expressed as Equation (3) and (4).

$$S_{av1} = \alpha \cdot S_{av} \quad (\varepsilon_c < \varepsilon \leq \beta\varepsilon_y) \tag{3}$$

$$S_{av2} = S_{av} \quad (\beta\varepsilon_y \leq \varepsilon) \tag{4}$$

Where, ε_c: strain of cracking strength, ε_y: strain of yield, $\beta\varepsilon_y$: strain when the Broms' intermediate cracks [5] is occurred as crack saturation state. The cracks before crack saturation state propagate when the strain reaches ε_c, and the Broms' intermediate cracks after crack saturation state propagate when the strain reaches $\beta\varepsilon_y$.

The effects of strain rate on strength of material are considered by the strength increase coefficient of concrete k_c and strength increase coefficient of steel bar k_s. The calculation of these two coefficients are expressed as Equation (5) and Equation (6) based on the literature [6].

$$k_c = (0.94 + 0.06 \cdot \log_{10}(\dot{\varepsilon})) \tag{5}$$

$$k_s = (0.9 + 0.05 \cdot \log_{10}(\dot{\varepsilon})) \tag{6}$$

Where, $\dot{\varepsilon}$: strain rate. The effects of strain rate on strain distribution is shown in Figure 17.

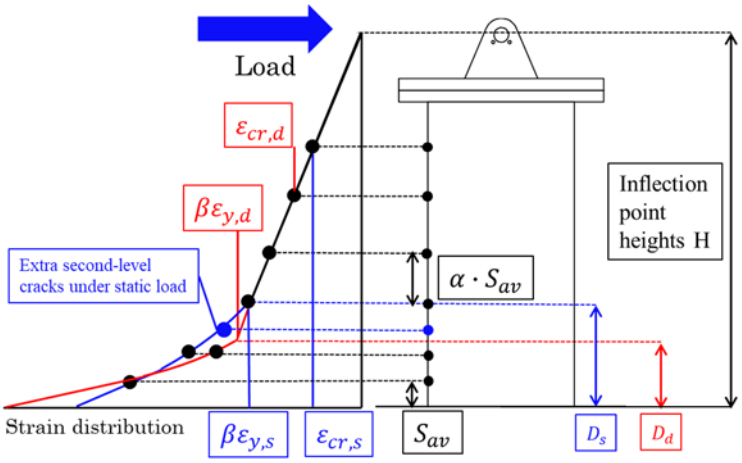

Figure 17 – Strain distribution of member under static load and dynamic load.

Based on the experimental results in Chapter 3, the crack saturation state judged by the strain on concrete surface by DIC gives the measurement result of rebar strain. There are estimated as 2070μ under static loading, and 3310μ under dynamic loading. These strain values mean the strain $\beta\varepsilon_{y,s}$ under static loading and $\beta\varepsilon_{y,d}$ under dynamic loading in Figure 17, respectively.

5. Applying the proposed method to another full-scaled R/C frame shaking table test

5.1 Outline of the shaking table test for RC frame

To verify the proposed method in the former chapter, another full-scaled R/C frame shaking table test [7] is employed. The plan of the 4-story R/C structure is shown in Figure 18. The specimen is designed to be 3000mm in floor height, 7200mm ×2 span at X direction, 7200mm ×1 span at Y direction with shear force wall settled.

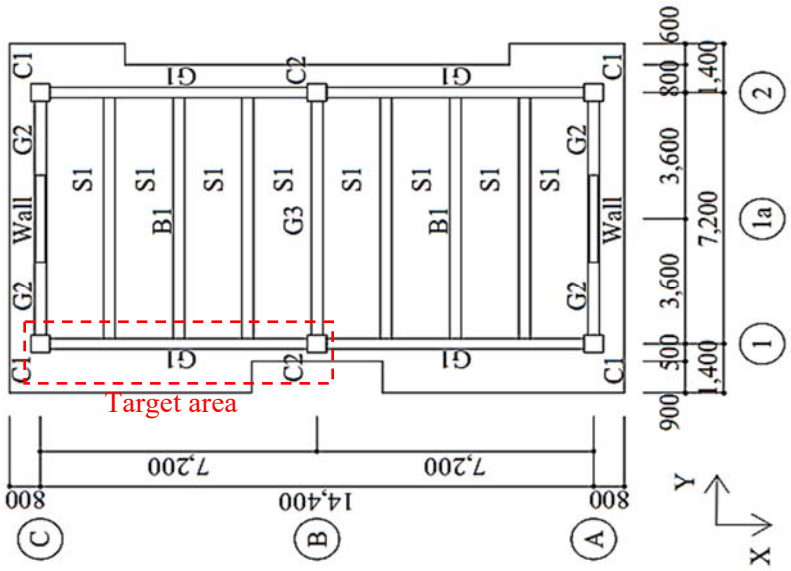

Figure 18 – Plan of 2nd to 4th floor [mm]

The beams G1 of 2nd floor to 3rd floor and the center column C2 and side column C1 of the 1st floor to the 2nd in the area marked in Figure 18 are the target structural members to estimate the damage in this research. The cross section, bar arrangement and material strength are shown in Table 5.

Table 5 – Material property and rebar arrangement detail

	1F	2F
G1		
Top rebar	6-D22	5-D22
Bottom rebar	3-D22	
Stirrup	2-D10@200	
B x *D*[mm]	300 x 600	
C1		
Rebar	10-D22	8-D22
Hoop	3,4-D10@100	2,3-D10@100
C2		
Rebar	10-D22	
Hoop	3,4-D10@100	2,4-D10@100
B x *D*[mm]	500 x 500	
rebar diameter	D22	D10
σ_y[N/mm^2]	370	388
σ_r[N/mm^2]	555	513
σ_B[N/mm^2]	39	

The JMA-Kobe wave is loaded with amplitude multiplied 10%, 25%, 50%, 100%, respectively. And the JR-Takatori wave is loaded with amplitude multiplied 40% and 60%. The damage of Run4 (JMA-Kobe 100%; the maximum drift ratio 0.034[rad] at 1st floor and 0.031[rad] at 2nd floor) and the Run5 (JR-Takatori 40%; the maximum drift ratio 0.034[rad] at 1st floor and 0.032[rad] at 2nd floor) of the target structural members are estimated and discussed in this research.

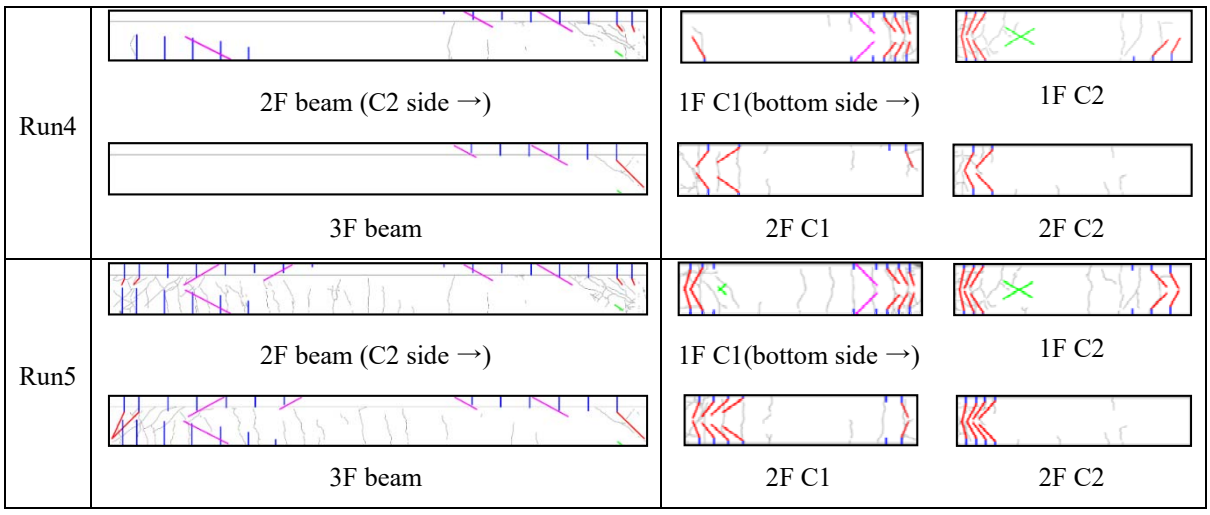

Figure 19 – Cracking pattern

5.2 Result of crack length estimation

Figure 19 shows the estimated cracking pattern and the observed cracking pattern at Run4 and Run5. Estimated crack length of 2nd floor beams are smaller than the result of 3rd floor at Run4 and Run5, which shows same tendency with result of observed crack length. But the estimated crack length shows larger value at Run4 and smaller value at Run5 than observed crack length. The reason of overestimate at Run4 is that proposed method assumes the displacement along each member are symmetry, while the actual displacement shows different results. The reason of underestimate at Run5 is that the tensile load of beams is not considered in the proposed method. Therefore, the plastic extending area is estimated smaller than actual situation, which makes the underestimate of crack number. The cracks caused by Y direction load and pull out of bar are not estimated in proposed method, which makes estimated crack length of 1st floor columns smaller than observed crack length at Run4 and Run5. The tendency and plastic extending area of observed result is reproduced well in estimated result.

6. Conclusions

The following findings are obtained in this research.

(1) When DIC is applied to strain distribution measurement nearby cracks occurring on the concrete surfaces, the optimal facet size is 0.5 times the strain gauge length. That brings the most approximate measurement results by strain gauge as a conventional method.

(2) Before the steady-state crack propagation, the tensile force and strain occurs on the concrete in the vicinity of the hair crack. After the steady-state crack propagation, the crack widens like between rigid elements.

(3) A method to change the average crack spacing according to the rebar strain distribution is proposed. By determining the relationship between the occurrence of primary cracks and secondary cracks and the rebar strain distribution, it is possible to roughly estimate the amount of crack damage after an earthquake.

(4) The strain under the dynamic loading is concentrated rather than that under static loading after a steady-state crack propagation

7. References

[1] Peters W, Ranson W (1982): Digital imaging techniques in experimental stress analysis, *Optical Engineering*, Vol.21(3), 427–431.

[2] Takahashi, N. (2017): Influence of loading ratio on quantified visible damages of R/C structural members, *Proc. of the Sixteenth World Conference on Earthquake Engineering*, Paper No.1458.

[3] Zhou, Y. and Takahashi, N. (2018): Simple estimation method of seismic damage quantification of full-scale RC frame, *Proceedings of the Japan Concrete Institute*, Vol.40, No.2, 853-858 (in Japanese)

[4] Architectural Institute of Japan (2004): *Guidelines for Performance Evaluation of Earthquake Resistant Reinforced Concrete Buildings* (in Japanese)

[5] B. B. Broms (1965): Crack Width and Crack Spacing in Reinforced Concrete Members, *ACI Journal*, No.62-67, 1237-1255

[6] Kaneko, T. (2002): *Effect of strain rate on the load-restoring force characteristics of RC beam*, University of Tokyo (in Japanese)

[7] T. Nagae, W. M. Ghannoum, J. Kwon, K. Tahara, K. Fukuyama, T. Matsumori, H. Shiohara, T. Kabeyasawa, S. Kono, M. Nishiyama, R. Sause, J. W. Wallace, J. P. Moehle (2015): Design implications of a large-scale shaking table test on a four-story reinforced concrete building, *ACI Structural Journal*, 112(2), 135-146

